Detector simulation and validation with dat

Abstract

We detail in this note the simulation method of the EASIER detector from the Radio Frequency (RF) signal to the ADC trace. We validate and compare our models with the data of the three different C-band detectors.

1 Expected signal

We present in this section the calculation of the expected signal. The main ingredients are:

- the sun flux (the sun flux varies with time)
- the sun path with respect to the antenna depending on the time of the year
- the antenna pattern

Given these ingredients can then calculate the expected increase of power collected output by the antenna and deduce the expected increase of the baseline for a given system temperature.

1.1 Sun flux

In our frequency range GHz, the sun flux has two main contributions [1]: a quiet sun component (or background component) with a constant intensity and a frequency dependence as:

$$Sq\ [SFU] = 26.4 + 12.4\ \nu + 1.11\ \nu^2 \text{for } (1 < \nu(\text{GHz}) < 20) \quad (1)$$

a second contribution, the so called slowly varying component, its spectrum is parameterised as:

$$Sv\ [SFU] = \frac{0.64(F10.7 - 70)f^{0.4}}{1 + 1.56(ln\ (\ f\ /\ 2.9))^2} \quad (2)$$

These spectra are shown in the figure 5 The intensity of the total flux at 2.8GHz (F10.7) is

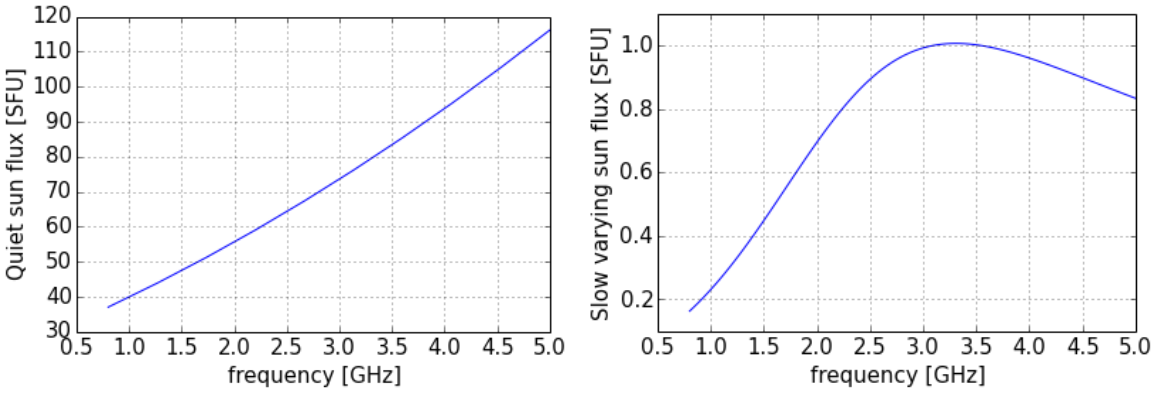

Figure 1 Left: quiet sun spectrum, Right: varying component spectrum

measured by several observatories[2], [3]. Making use of these data and the parameterization in frequency written above, one can deduce the flux in the C-band.

F10.7

sun path

expected signal

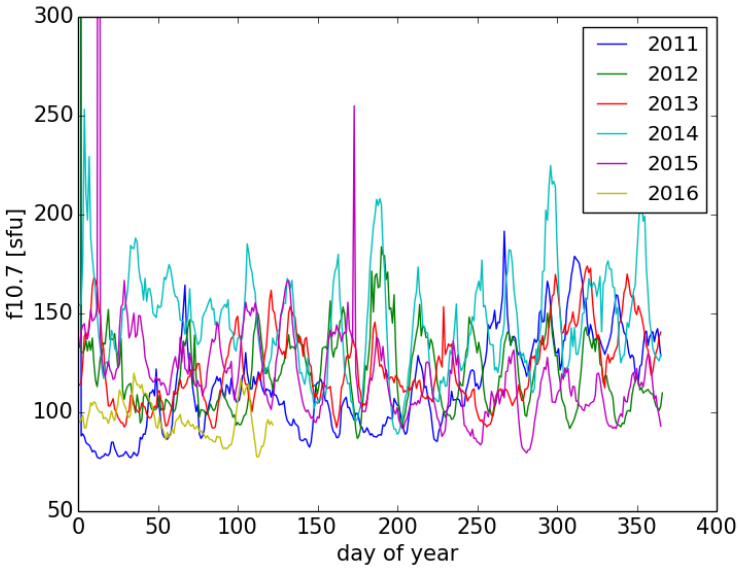

Figure 2 Left: quiet sun spectrum, Right: varying component spectrum

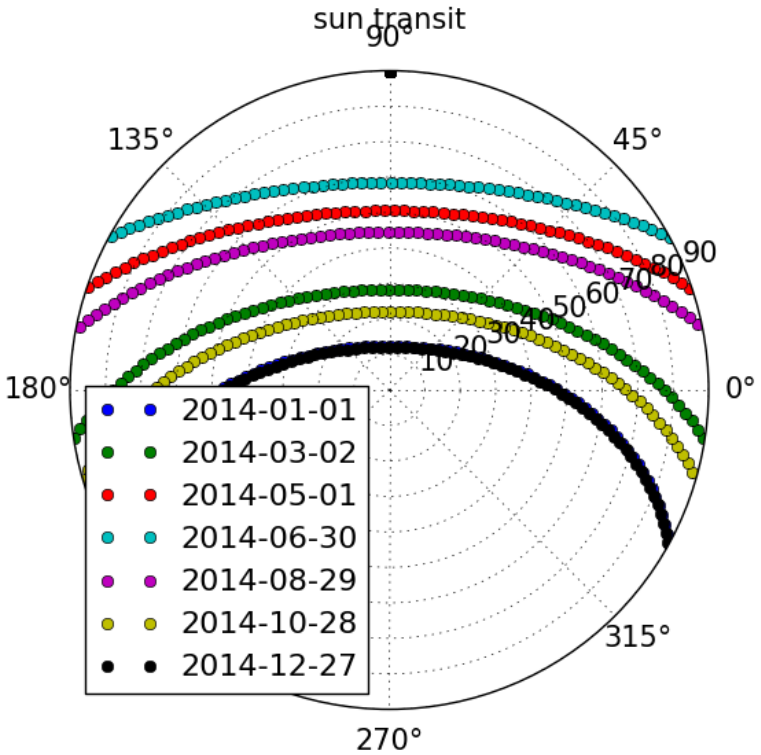

Figure 3 Left: quiet sun spectrum, Right: varying component spectrum

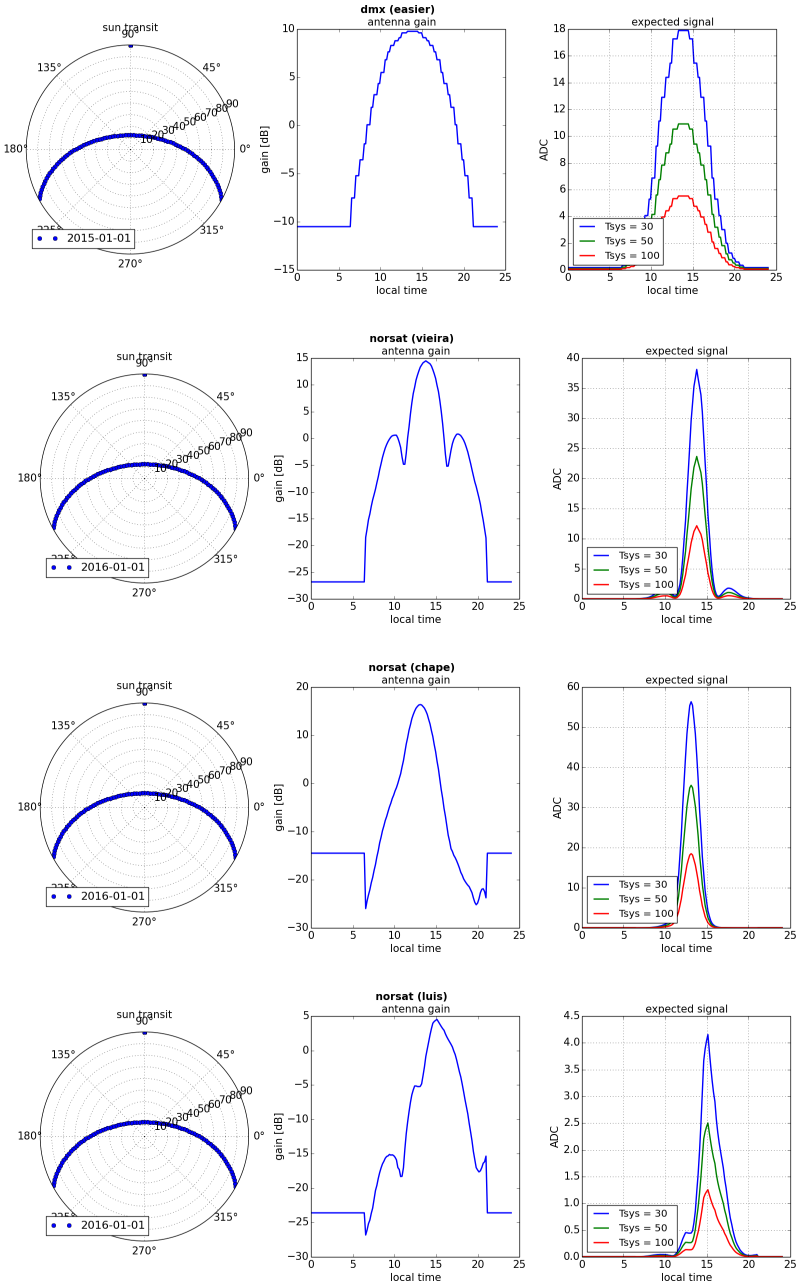

Figure 4 Left: quiet sun spectrum, Right: varying component spectrum

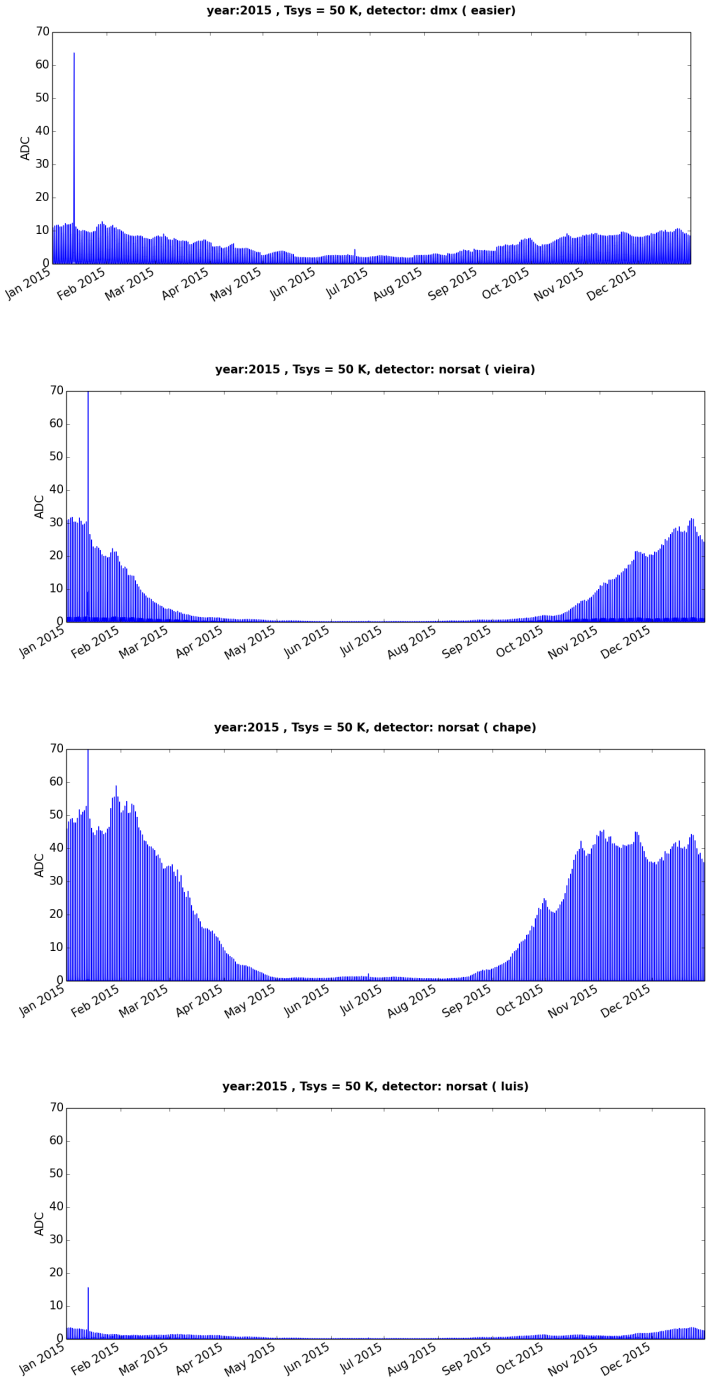

Figure 5 Left: quiet sun spectrum, Right: varying component spectrum

2 Data description and baseline parameterization

In this section we attempt to understand and parameterize the radio baseline. We will separe the various detectors EASIER7/EASIER61/GIGADuck. The first part describes the basic cut we apply, the second describes the baseline parameterization we can obtain. We analyse the monitoring data recorded every 400 second at the local station. The data contains the basic information on the radio trace, i.e. the average and the RMS. But we have also information from the Los Leones weather station, for instance the outside temperature and humidity.

2.1 a first look at the data and basic cuts 36

We expect the radio baseline to vary because of different sources:

- a variation of gain: a variation of gain is likely to happen with temperature. 38
- the microwave flux: if a source strong enough enters in the field of view of the antenna. This is what is expected for the sun flux. 40
- atmospheric effect: this is also a variation of the radio flux but it is due to absorption of clouds, or an increase of the field due to stormy conditions. 42

2.1.1 overview

We show the raw baseline over several time scales in the figure 6. We see two main modula-

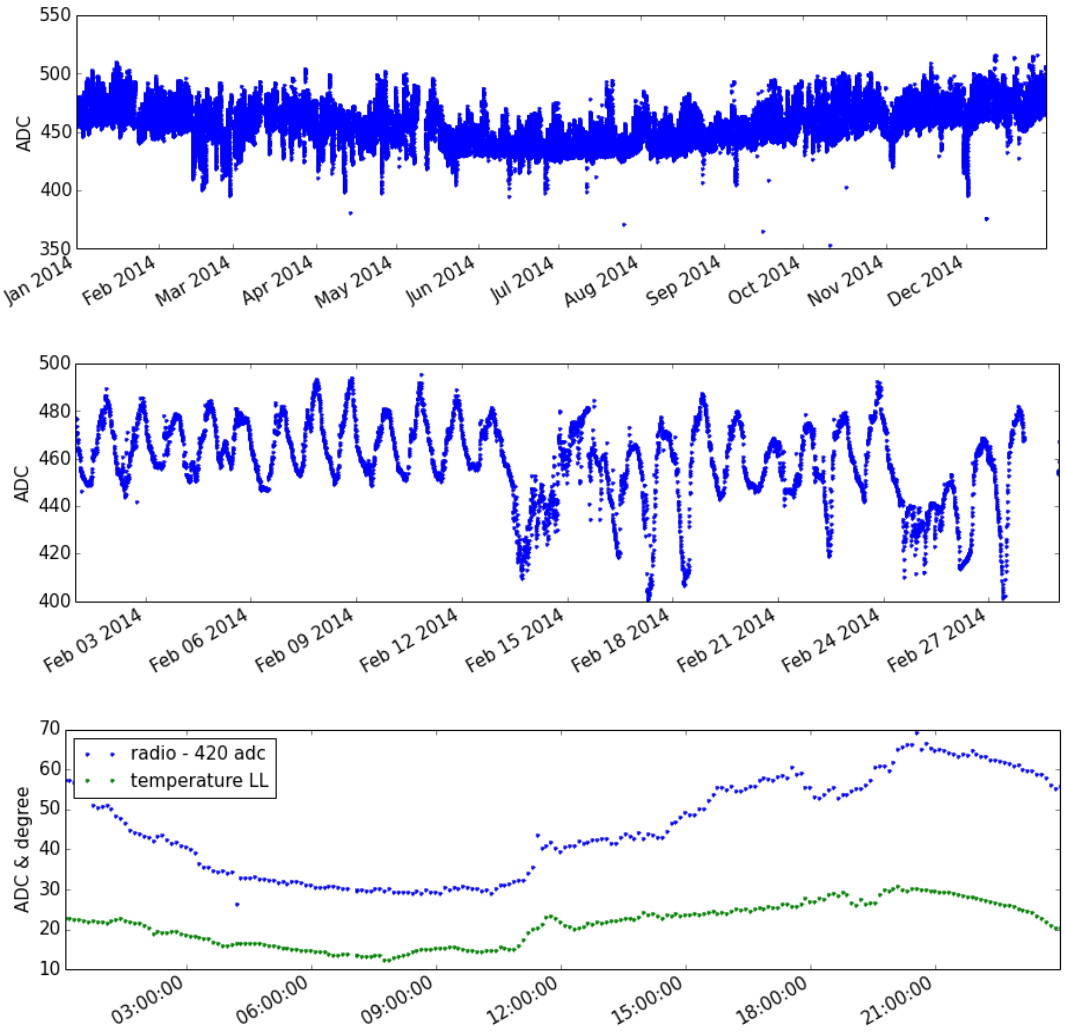

Figure 6 Left: quiet sun spectrum, Right: varying component spectrum 44

tions, a long term variation one on the year long plot, and a daily modulation on the month

long plot. We can also notice a large decrease of the baseline (i.e. increase of the radio power) for instance in the middle of February. We will see later that this can be related to rain. When there is no such rainy condition the typical spread of the baseline is around 40-50 ADC counts. However we notice clearly on the bottom plot of figure 6 the strong dependence with the outside temperature.

When we compare the 7 antennas over the same time period (see figure 7), we notice the structure has the same shape, but the amplitude of the variations can be very different: for instance stId332 has variations of the order of 30-40 ADC counts and stId 342 has variations of the order of 150 ADC counts) In my opinion, these differences are due to a different

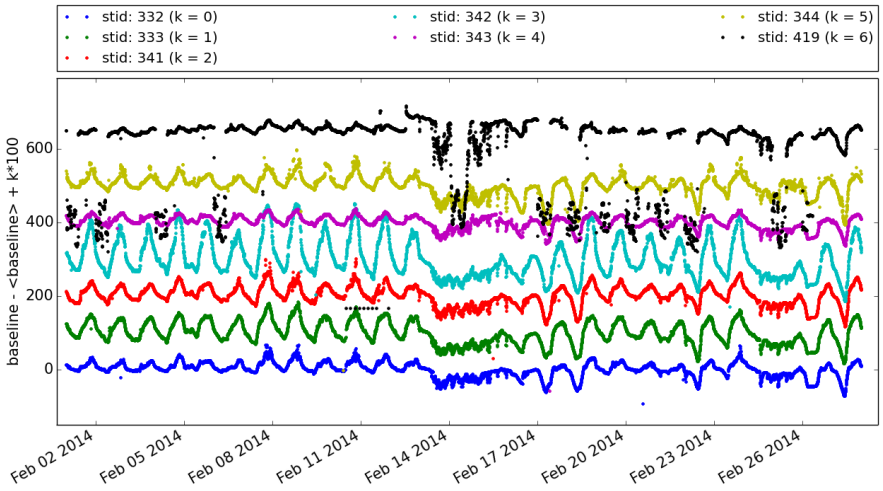

Figure 7

dependence of the gain with the temperature. The gain itself is not related to the system temperature, but it shows that the 7 LNBf might have different characteristics.

2.1.2 cuts

humidity We have just seen that some periods look very different, see for instance around February 15 in the fig 6. These large baseline seem to be related to the rain. Figure 8 show the baseline together with the humidity percentage measured with Los Leones weather station. It is clear that a humidity larger than 60/70 % has a strong effect on the baseline. This effect is more a threshold effect than a correlation: when it rains we can't trust the baseline. In the following we require the humidity to be less than 50 %.

sun/no sun periods The sun is expected to give a contribution to the baseline. We need to exclude the period when a significant signal is expected in order to keep this effect. The sun/no sun periods are determined with the expected signal calculated above. We assume a temperature of 50K for the detector and consider a signal above 5 ADC count as significant. The figure 9 is an example of the split of the data in sun/no sun period (also after the humidity cut).

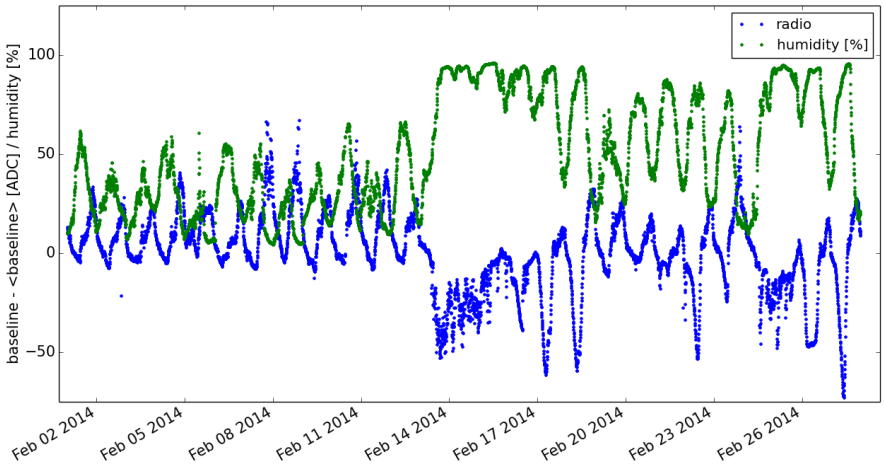

Figure 8

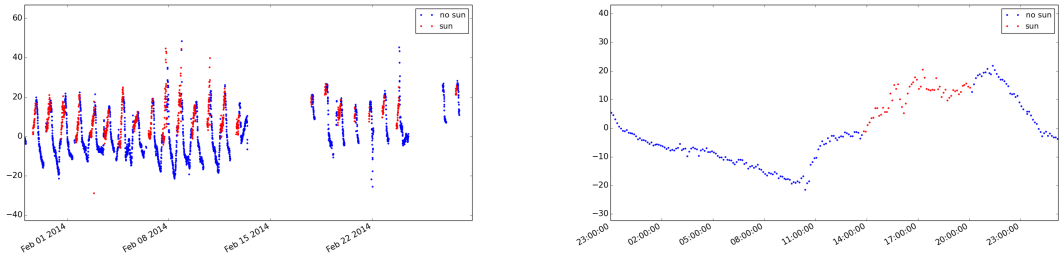

Figure 9

long term variation We have seen that there is a long term modulation of the baseline. To remove this dependence we filter out the low frequencies (below one day).

2.2 Temperature parameterization

The radio baseline is strongly dependent on the outside temperature. The figures 10 shows the baseline against the temperature for one year of data of the stations 332 and 342. This can be explained by a variation of the LNB gain with the temperature [4]. When we perform a linear fit and correct the baseline with this function, we obtain a baseline distribution with a spread of 5 to 16 ADC depending on the station.

If we perform a daily fit of the temperature dependence we can obtain a better correction of the baseline. We show in the figure 11 the fits for each day on the left and the resulting corrected distribution on the right. We see that the fits can be very different depending on the day, meaning that other parameters are not accounted for.
Furthermore, we want to be able to compare a *non sun* hypothesis with a *sun* hypothesis, so we need a prediction of the baseline during the time we expect the sun (the sun signal

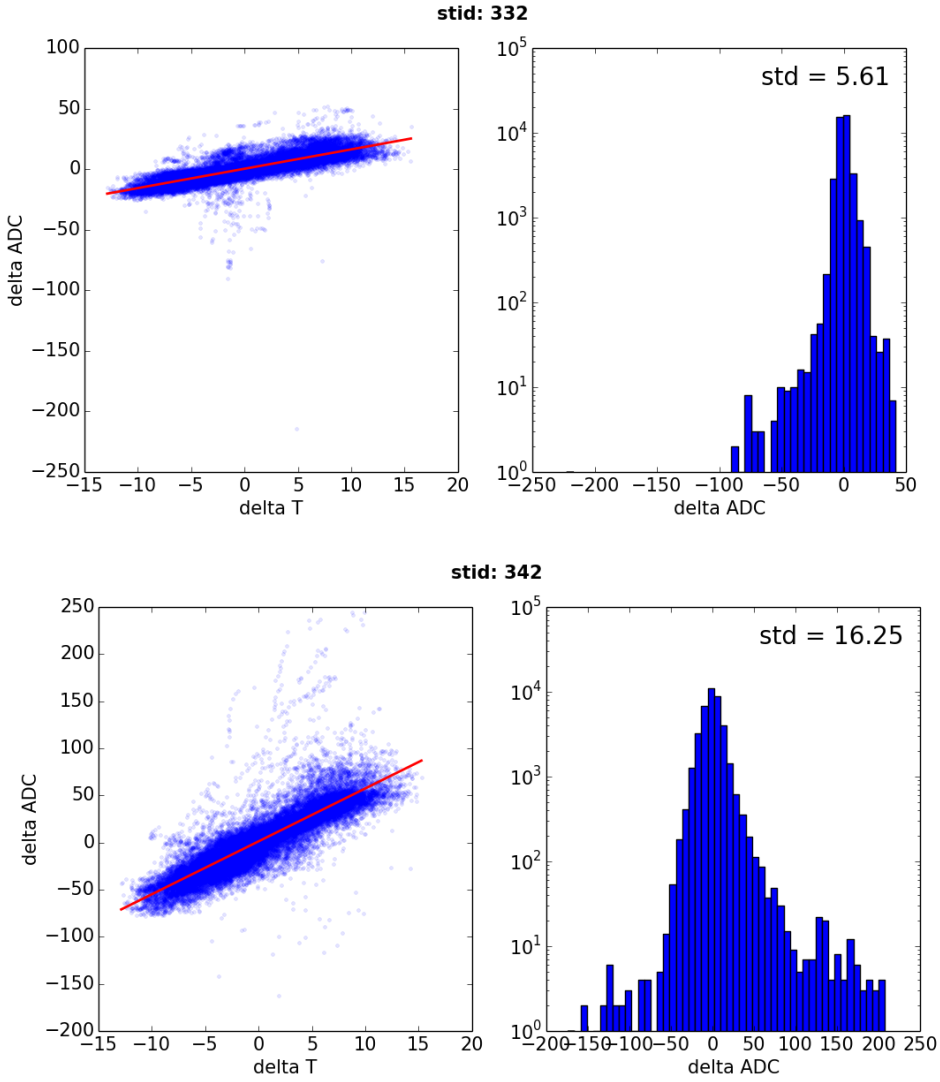

Figure 10

is expected usually between 11h00 and 16h00 in local time, i.e. 14h00 and 19h00 in UTC). In the figure 13 we show the baseline comparison of the baseline between 14:00 and 19:00 for the days we don't expect the sun signal.

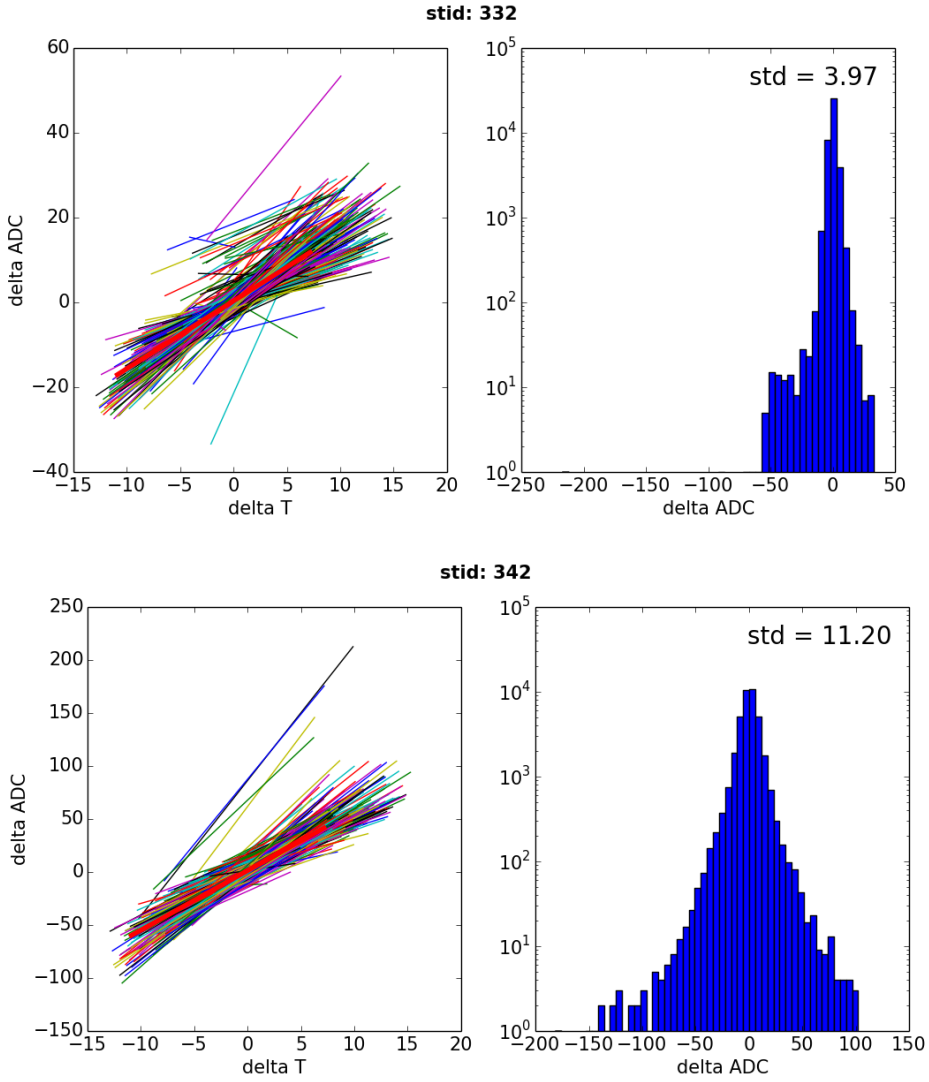

Figure 11

2.3 GIGADuck

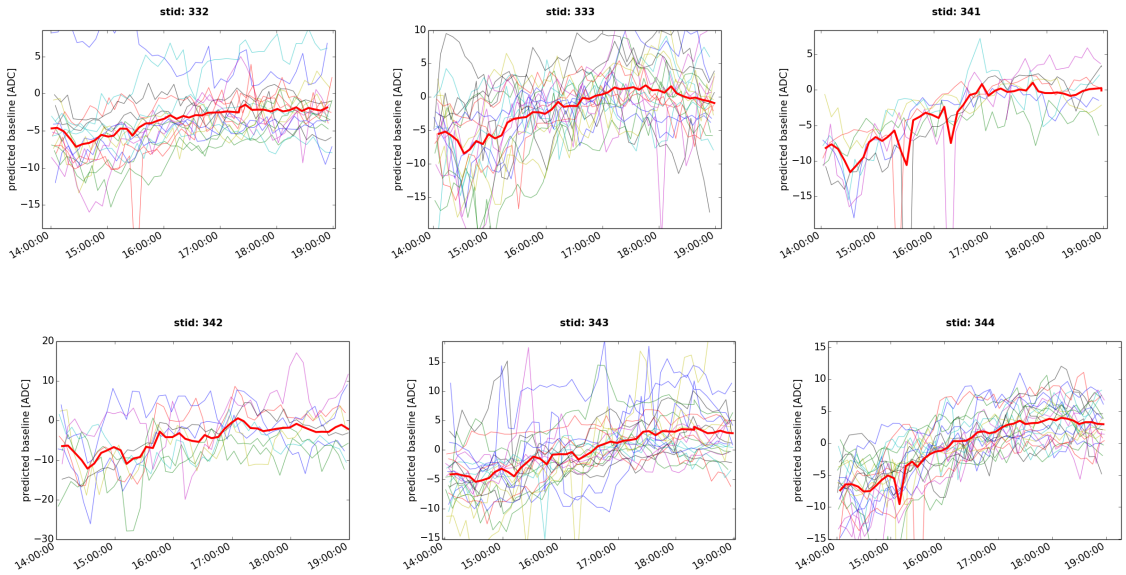

Figure 12 baseline prediction with the temperature fit over a year

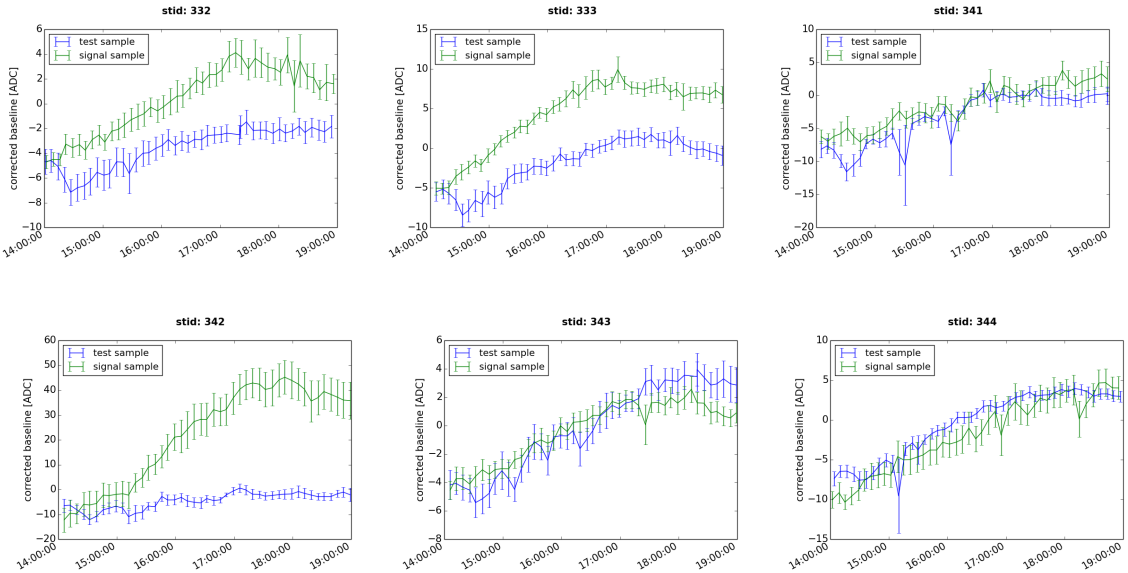

Figure 13 baseline prediction with the temperature fit over a year

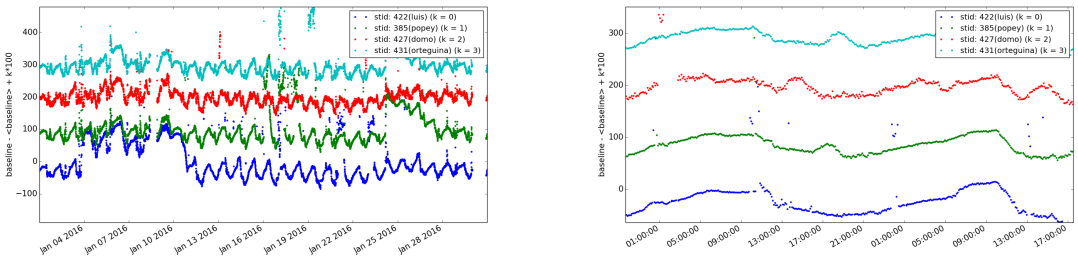
stid: 422(luis) (k = 0)
stid: 385(popey) (k = 1)
stid: 427(domo) (k = 2)
stid: 431(orteguina) (k = 3)
baseline - <baseline> + k*100
Jan 04 2016
Jan 07 2016
Jan 10 2016
Jan 13 2016
Jan 16 2016
Jan 19 2016
Jan 22 2016
Jan 25 2016
Jan 28 2016
01:00:00
05:00:00
09:00:00
13:00:00
17:00:00
21:00:00

Figure 14

References 88

[1] *http://www.spaceacademy.net.au/spacelink/solrfi/solrfi.htm*, .

[2] *Nobeyama Radio Observatory (http://solar.nro.nao.ac.jp/norp/html/policy$_n$ew.html)*, .

[3] *Nasa Space Physics Data Facility (http://omniweb.gsfc.nasa.gov/form/dx1.html)*, . 90

[4] P. Stassi, *TechEAS 06A - Dependances en temperature 08fev12.pdf*, .